Supporting Information

Kong et al. 10.1073/pnas.1311289110

SI Text

Tissue Samples

The samples were kept frozen at -20 °C until used for Raman spectral measurements. "Tissue block" refers to tissue layers thicker than 0.5 mm removed during MMS. "Tissue sections" represent skin sections of 20 μm thickness cut from tissue blocks with a microtome (CM1900 UV, Leica). Tissue blocks were excised by the Mohs surgeon, embedded within optimal cutting temperature medium (OCT), and frozen with a cryogenic spray (Frostbite, Surgipath). For each tissue block, a section was cut and H&E stained for gold standard diagnosis by histopathology (called adjacent section). The remaining tissue block was then washed and fully defrosted for Raman spectral measurements. After the Raman spectroscopy measurements, the skin sections were stained by haematoxylin and eosin (H&E) and the diagnosis was provided by two Mohs surgeons and a consultant histopathologist. Only samples for which the diagnoses provided by the surgeons and histopathologist agreed were included in the study. For Raman measurements of tissue blocks, the samples were deposited on MgF_2 coverslip (0.17 mm thick) and were maintained in phosphate buffer saline (PBS) during the measurements. In total, samples from 115 patients with BCC on the face or neck were included in this study.

Raman Spectroscopy and Autofluorescence Imaging

The Raman spectra were recorded using a custom-built Raman microspectrometer based on an inverted optical microscope (Eclipse Ti; Nikon) with a 50×/0.55 objective (Leica), 785-nm wavelength laser (StarBright XM; Torsana), spectrometer (77200; Oriel), back-illuminated deep-depletion CCD (DU401-A-BR-DD; Andor Technology), and automated sample stage (H107 ProScan II; Prior Scientific). The wavelength of the excitation laser was selected to minimize the excitation of tissue autofluorescence. The acquisition time for the Raman measurements was 2 s per position, and the laser power at the sample surfaces was 200 mW. The spectrometer was calibrated using naphthalene and 1,4-bis(2-methylstyryl) benzene samples (both from Sigma–Aldrich) to an accuracy of 0.5 cm^{-1}. The autofluorescence images of tissue sections were measured using a wide-field fluorescence imaging system integrated into the Raman microscope; the system consisted of a mercury lamp (Nikon), CCD camera (01-QIClick-F-M-12 Mono; QImaging), and fluorescence filters for collagen (DAPI-5060C-NTE-ZERO; Semrock) and tryptophan (FF310-Di01-25 × 36, FF01-292/ 27–25, FF01-357/ 44–25; Semrock). For tissue blocks, the autofluorescence images were recorded using a separate confocal fluorescence microscope equipped with a 457.9-nm laser (C1; Nikon).

The following preprocessing procedures were applied to all Raman spectra: removal of cosmic-ray peaks, subtraction of the background Raman signal of the microscope objective and MgF_2 substrate, subtraction of a baseline based on a rubber band method (the rubber bands were chosen between the regions 750–850 cm^{-1}, 855–950 cm^{-1}, 951–1,050 cm^{-1}, 1,135–1,254 cm^{-1}, 1,488–1,600 cm^{-1}, and 1,675–1,750 cm^{-1}), and normalization to zero mean and unit variance.

Several data reduction methods [10 principal components, 10 principal components followed by the multiclass linear discriminant analysis (LDA) rank reduction, ratios of band areas] and classification techniques (LDA, quadratic discriminant analysis, multinomial logistic regression) were compared based on a five-fold cross-validation algorithm (the dataset was split in groups of 11 patients). All classifiers were tuned to the regime providing 95% sensitivity on the training data. Then, the models were tested using an independent set of tissue samples from new patients. The model with the best classification performance for BCC diagnosis was then selected and used further in the study.

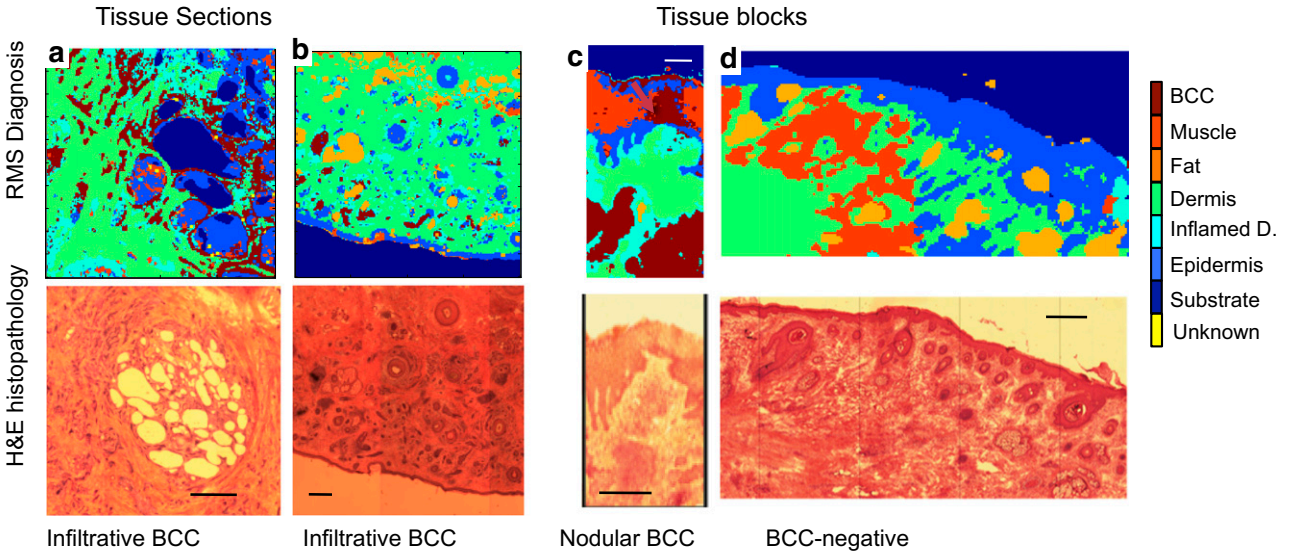

Fig. S1. Quantitative diagnosis by Raman microspectroscopy using raster scanning for tissue sections and unsectioned tissue blocks. Tissue sections: (*A* and *B*) infiltrative basal cell carcinoma (BCC). Unsectioned tissue layers: (*C*) nodular BCC; (*D*) BCC-negative. The histopathology images for adjacent sections are included for comparison. (Scale bars: 400 μm.) False positives are indicated by red arrows.

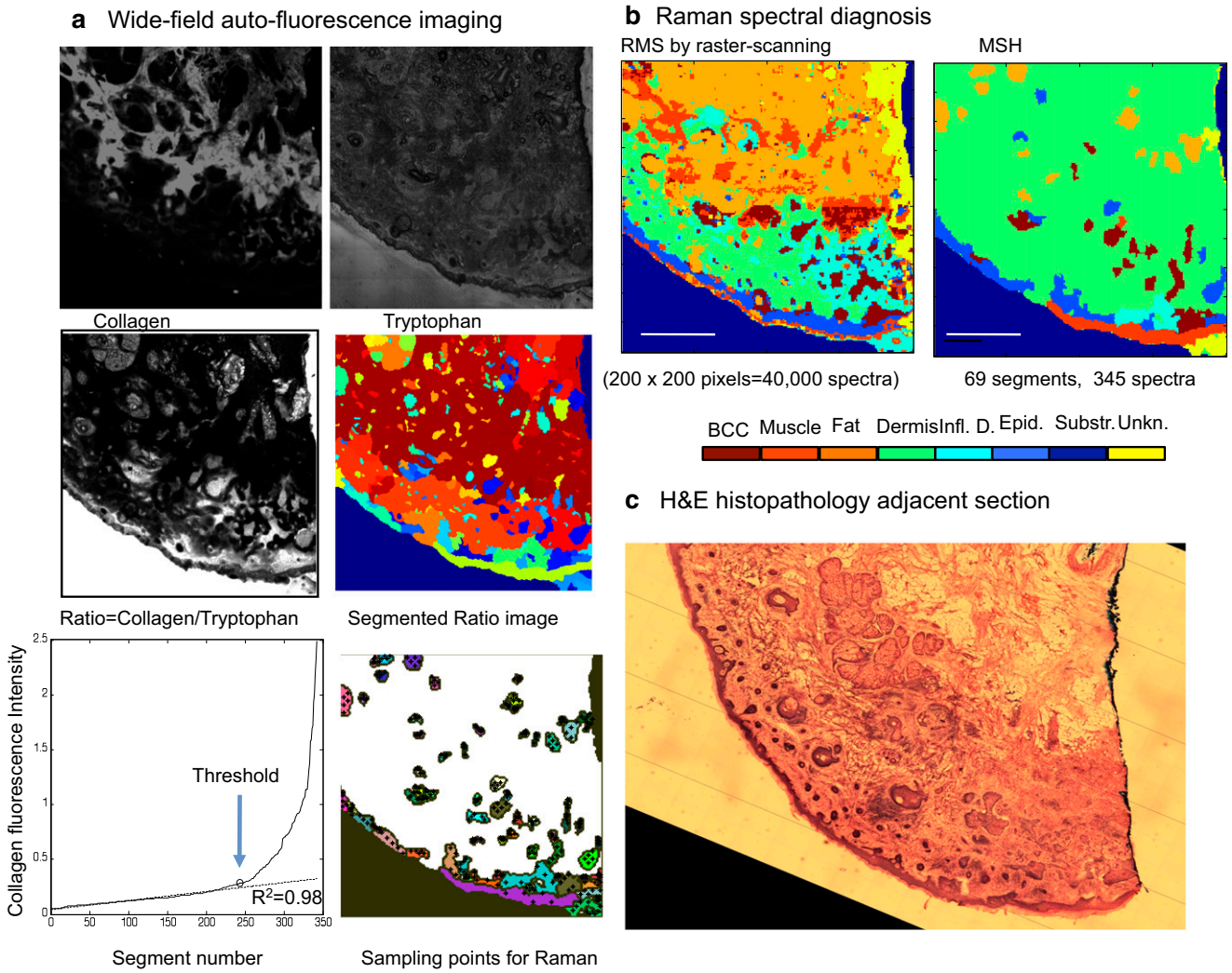

Fig. S2. Comparison between BCC diagnosis obtained by multimodal spectral histopathology (MSH) and by raster-scanning Raman spectroscopy. (*A*) Use of tissue autofluorescence images to determine sampling points for Raman spectroscopy measurements in MSH. Segments above the threshold in the collagen autofluorescence image are classified as dermis and excluded from the Raman spectra measurements. (*B*) Diagnosis obtained by 200 × 200 raster-scanning Raman spectroscopy (40,000 spectra) compared with the MSH diagnosis using 350 spectra, as indicated in the segmented image. (*C*) Histopathology image of the adjacent tissue section. (Scale bars: 0.5 mm.)

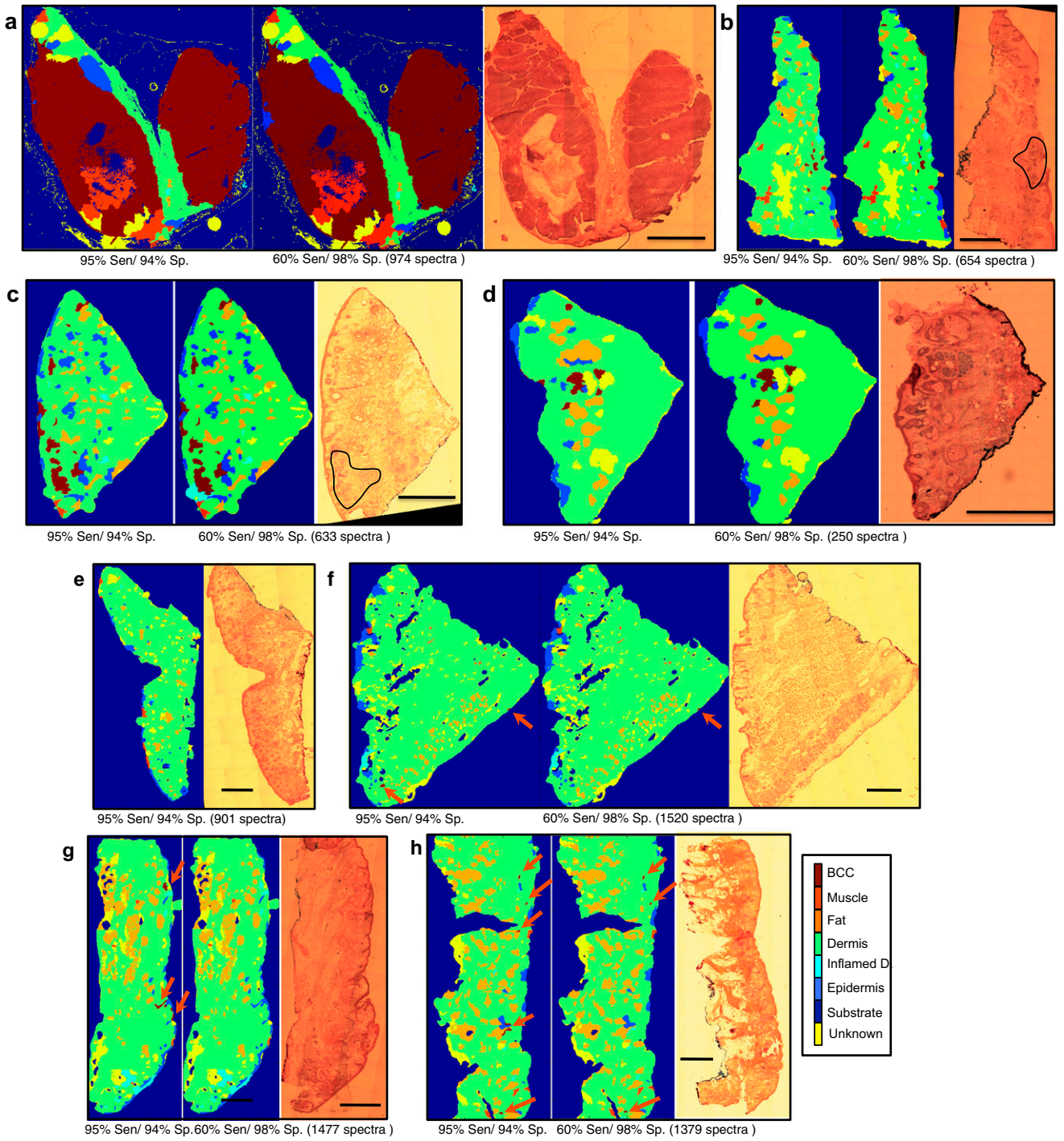

Fig. S3. MSH diagnosis for the skin sections in Fig. 4 corresponding to the high (95% sensitivity and 94% specificity) and low (60% sensitivity and 98.8% specificity) sensitivity regimes per spectrum. (Scale bars: 2 mm.) (*A–D*) BCC-positive samples, (*E–H*) BCC-negative samples (red arrows indicate the false positive segments).

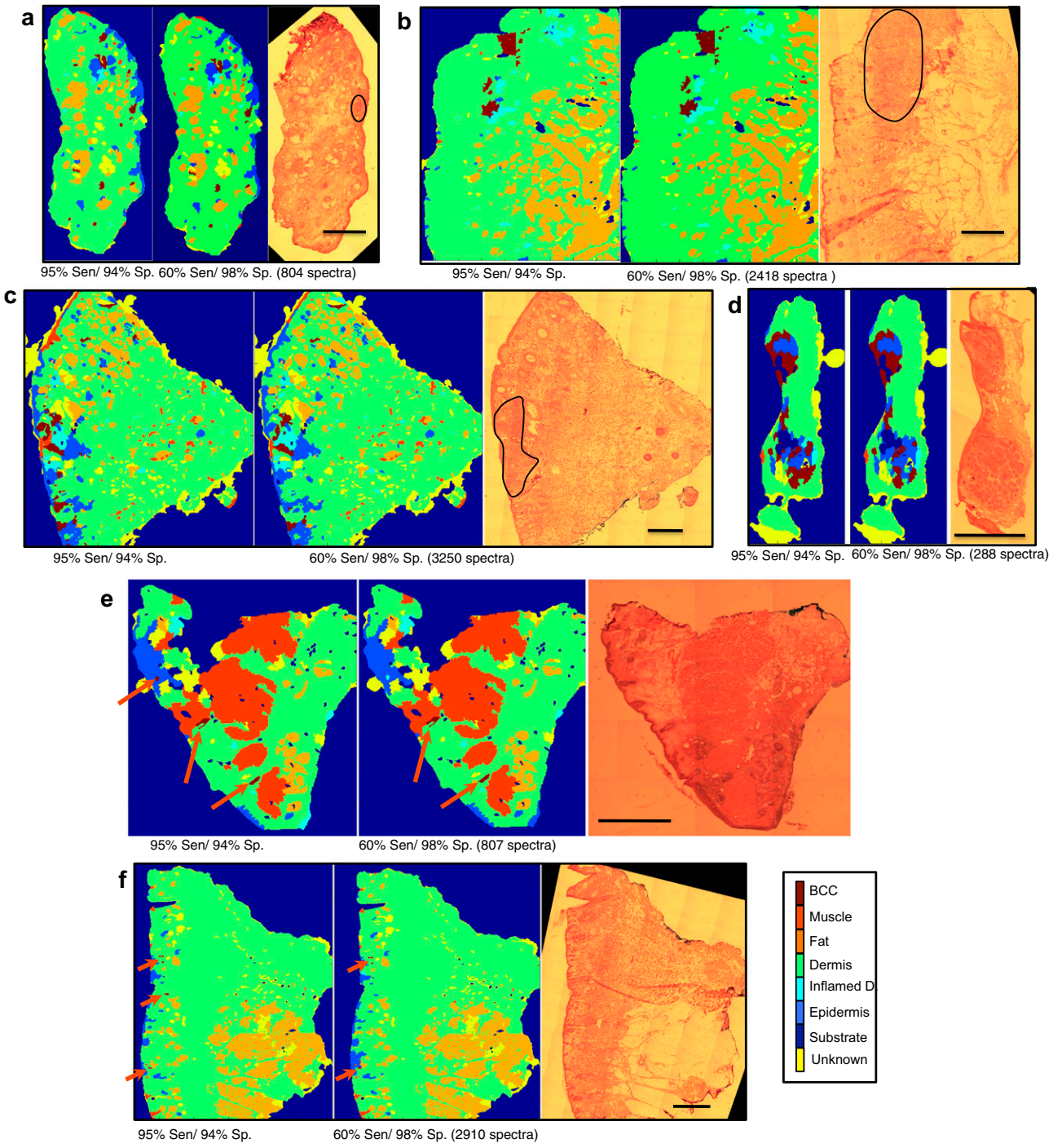

Fig. S4. MSH diagnosis for tissue sections from patients with BCC on the face or neck. (*A*–*D*) BCC-positive samples. (*E* and *F*) BCC-negative samples (red arrows indicate the false positive segments). The diagnostic images were obtained by setting the classification models at two target sensitivity levels for BCC: 95% sensitivity and 94% specificity (95% Sen/94% Sp.), and 60% sensitivity and 98.8% specificity (60% Sen/98% Sp.). The number of spectra measured for every sample is included in brackets and is the same for both diagnostic regimes. Histopathology images for adjacent sections are included for comparison, and areas of the BCC are highlighted by black curves where appropriate. (Scale bars: 2 mm.)

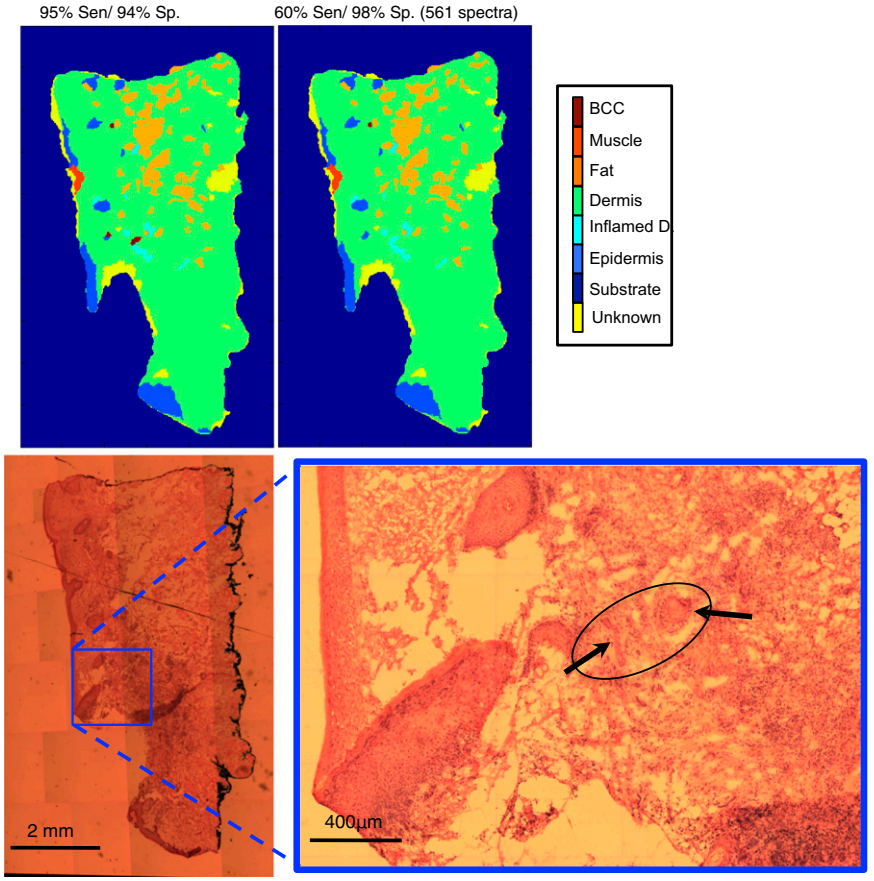

Fig. S5. BCC sample for which MSH provided the correct diagnosis in the high-sensitivity regime (95% sensitivity, 94% specificity) and false negative diagnosis in the low-sensitivity regime (60% sensitivity, 98% specificity). The tumor regions are indicated by black arrows.

Table S1. Confusion matrix for the independent validation of the Raman classification model at target sensitivity 95%

	Unk.	BCC	Epid.	Infl.	Derm.	Fat	Musc.
Unk.	0	0	0	0	0	0	0
BCC	0	100	0	0	0	0	0
Epid.	0	16.7	80.0	3.3	0	0	0
Infl.	0	16.7	0	33.3	50	0	0
Derm.	0	2.0	0	9.8	88.2	0	0
Fat	0	0	0	0	0	100	0
Musc.	0	0	18.2	0	0	0	81.8

Values represent percentages. Derm., dermis; Epid., epidermis; Infl., inflamed dermis; Musc., muscle; Unk., unknown.